123

Compressed Genotyping

Yaniv Erlich, Assaf Gordon, Michael Brand, Gregory J. Hannon and Partha P. Mitra

Abstract— Significant volumes of knowledge have been accumulated in recent years linking subtle genetic variations to a wide variety of medical disorders from Cystic Fibrosis to mental retardation. Nevertheless, there are still great challenges in applying this knowledge routinely in the clinic, largely due to the relatively tedious and expensive process of DNA sequencing. Since the genetic polymorphisms that underlie these disorders are relatively rare in the human population, the presence or absence of a disease-linked polymorphism can be thought of as a sparse signal. Using methods and ideas from compressed sensing and group testing, we have developed a cost-effective genotyping protocol. In particular, we have adapted our scheme to a recently developed class of high throughput DNA sequencing technologies, and assembled a mathematical framework that has some important distinctions from 'traditional' compressed sensing ideas in order to address different biological and technical constraints.

I. INTRODUCTION

Genotyping, the process of determining the genetic variation of a certain trait in an individual, has become a pivotal component of medical genetics, as a broad spectrum of disorders are now known to be induced by non-functional genes. In the past thirty years, extensive efforts were made to identify and locate risk alleles of severe genetic diseases, which are characterized by incapacities or lethality of the affected individuals at an early age, and very low prevalence in the population. These efforts have not only led to deeper insights regarding the molecular mechanisms that underlie those genetic disorders, but have also contributed to the emergence of large scale genetic screens, where individuals are genotyped for a panel of risk alleles in order to detect genetic disorders and provide early intervention where possible.

Genetic diseases are broadly classified into two groups according to the effect of the underlying mutation - either *dominant* or *recessive*. This classification is elucidated by the diploidy of the human genome, meaning that each gene appears in two copies (except the X and Y chromosomes in male). Dominant mutation induces a disorder even when present only on one chromosome, whereas recessive mutation induces the disorder only if both copies are non-functional. Thus, for a disease caused by a recessive mutation, individuals are classified into three groups : (a) *normal* if their two alleles are intact, (b) *carriers* if only one allele is functional (c) *affected* if their two alleles are non-functional. Table I illustrates this classification. A *carrier screen* is a genetic test for detecting individuals that are heterozygous with respect to

a risk allele of a severe genetic disease. If two carriers bread, they have 25% chance of having an affected offspring for each carriage, and in some countries that face high prevalence of severe genetic diseases the practice is to offer a screen to the entire population, regardless their familial history for early monitoring and prevention [1], [2]. Therefore, due to the importance and ubiquity in medical gentics and the intriguing connection to the theory of sparse signal recovery, our work is focused on carrier screens. However, large parts of the framework can be used also for other types of genetic screens.

The most common genotyping method is based on sequencing the regions that encompass the risk genes and analyzing the type of the DNA sequence - whether it matches the wild type (WT) alleles or a known risk allele. This approach gained popularity due to its high accuracy (sensitivity and specificy), applicability to a wide variety of genetic disorders, and technical simplicity. However, the current DNA sequencing technologies used for genotyping provide only serial processing of one specimen/region combination at a time. This increases the cost of labor and other expenses in large-scale screens and essentially deters individual participation and limits the panel of genes that are analyzed.

Recently, a new class of DNA sequencer methods, dubbed *next-generation sequencing technologies* (NGST) has emerged, revolutionizing molecular biology and genomics (reviewed in [3]–[5]). These sequencers process the DNA fragments in parallel and provide millions of sequence reads in a single batch, each of which corresponds to a DNA molecule within the sample. While there are several types of NGST platforms and different sets of sequencing reactions, all platforms achieve parallelization using a common concept of immobilizing the DNA fragments to a surface, so that each fragment occupies a distinct spatial position. When the sequencing regants are applied to the surface, they generate optical signals dependent on the DNA sequence, which are then captured by a microscope and processed. Since the fragments are immobilized, successive signals from the same spatial location convey the DNA sequence of the corresponding fragment (Fig. 1a). However, the spatial locations of the DNA fragments are completely random and are based on stochastic hybridization of a small aliquot (millions) of DNA fragments out of significantly larger number present in a sample. Therefore, if a DNA library is composed of multiple specimens, it is not possible to associate the sequence reads with their corresponding specimens. This limitation is the main obstacle to the utilization of next generation sequencers in large scale screens, since dedicating a run to each specimen is not cost effective.

A simple solution to overcome the specimen-multiplexing problem is to append unique identifiers, dubbed *DNA barcodes*, to each specimen prior to sequencing [6] [7]. These

Y. E, A.G, G.J.H, and P.P.M are with the Watson School of Biological Science, Cold Spring Harbor Laboratory, NY, 11724 USA M.B. is with Lester Associates, Bentleigh East, 3165 Australia

Email addresses: Y.E is in erlich@cshl.edu, A.G is in gordon@cshl.edu, M.B is in ieee@brand.scso.com, G.J.H is in hannon@cshl.edu, and P.P.M is in mitra@cshl.edu

TABLE I
GENOTYPE-PHENOTYPE CONNECTIONS IN GENETIC DISORDERS

Alleles	Genotype	Dominant Disorder	Recessive Disorder
AA	Homozygous WT	Normal	Normal
Aa	Heterozygous	Affected	Carrier
aa	Homozygous mut.	Affected	Affected

A - normal allele, a - mutant allele

barcodes are short DNA molecules that are artificially synthesized, and when attached to the DNA fragment, they label it with a unique sequence. The sequencer reads the entire fragment, and reports the sequence of the barcode with the sequence of the interrogated region. By reading the portion of the sequence corresponding to the barcode, the experimenter can associate a genotyped fragment to a given specimen (Fig. 1b). While this method was found quite successful for genotyping several dozens of specimens, the synthesis and ligation of large number of DNA fragments is both cumbersome and expensive. This restricts the scalability of the method for genetic screens that consist of thousands of individuals. In fact, with the current costs of synthesizing so many DNA barcodes, it is more cost beneficial to use the legacy serial-based DNA sequencers.

Drawing inspiration from compressed sensing [8], [9], we ask: *since only a small fraction of the population are carriers of a severe genetic disease, can one employ a compressed genotyping protocol to identify those individuals?* We suggest a protocol in which one genotypes pools of specimens on a next-generation sequencing platform that would approach the sequencing capacity, while reducing the number of barcodes and maintaining a faithful detection of the carriers.

A. Related work

Our work closely relates to group testing and compressed sensing, which deals with efficient methods for extracting sparse information from a small number of aggregated measurements. Much of the group testing literature (thoroughly reviewed in: [10], [11]) is dedicated to the *prototypical problem*, which describes a set of interrogated items that can be in an active state or an inactive state and a test procedure, which is performed on pools of items, and returns 'inactive' if all items in the pool are inactive, or 'active' if at least one of the items in the pool is active. Mathematically, this type of test can be thought of as an OR operation over the items in the pool, and is called *superimposition* [12]. In general, there are two types of test schedules: adaptive schedules, in which items are analyzed in successive rounds and re-pooled from round to round according to the accumulated results, and non-adaptive schedules where the items are pooled and tested in a single round. While in theory adaptive schedules require less tests, in practice they are more labor intensive and time consuming due to the re-pooling steps and the need to wait for the test results from the previous round. For that reason, non-adaptive schedules are favored, and have been employed for several biological applications including finding sequencing

tagged sites in yeast artificial chromosomes (YAC) [13] , and mapping protein interactions [14].

Compressed sensing [8], [9] is a recently emerged signal processing technique that describes conditions and efficient methods for capturing signals that are sparse in some orthonormal representation by measuring a small number of linear projections. This theory extends the framework of group testing to the recovery of hidden variables that are real (or complex) numbers. Additonal deviation from group testing is that the aggregated measurements reports the linear combination of the data points and not superimposition. However, some combinatorial concepts in group testing were found useful also for compressed sensing, and it has been recently shown that deterministic designs based on group testing can confer sublinear reconstruction runtimes for real signals [15]–[17]. The framework of compressed sensing was also found useful for applications beyond 'traditional' signal processing and recently a novel biological application was suggested - designing highly efficient microarrays that reduces the number of DNA probes, which is a factor hampering their miniaturization [18], [19].

Our approach combines lessons from both fields but also has key differences from these frameworks. The most obvious deviation of our is that rather than focussing solely on maximal reduction in the number of *queries* (termed 'measurements' in compressed sensing, or 'tests' in group testing) additional cost functions are introduced. Principally, we are interested in an additional objective of minimizing the weight of the design, corresponding to the number of nonzero elements of the design matrix (for a fixed number of specimens). This constraint originates from the properties of next generation sequencers, and prevents maximal query reduction. We will discuss the consequences of this constraint and provide some theoretical bounds and efficient designs. In particular, this theoretical framework is built on our recent experimental results regarding genotyping thousands of bacterial colonies using combinatorial pooling with NGSTs for a biotechnological application [20]. Prabhu et al. [21] develop a closely related theoretical approach to detect singletons using error correcting codes. A somewhat similar compressed sensing approach has been independently developed by Shental et al. [22].

The manuscript is divided as follows: In section II, we set up the basic formulation of compressed genotyping. In section III, we present the concept of light-weight designs and provide a lower theoretical bound. Then, we show how constructions based on the Chinese Reminder Theorem comes close to this bound. In section IV, we present a Bayesian reconstruction approach based on belief propagation, and in section V, we provide several simulations of carrier test, including Cystic Fibrosis. Section VI concludes the manuscript.

II. THE GENOTYPING PROBLEM - PRELIMINARIES

A. Notations

We denote matices as an upper-case bold letter and the (i, j) element of the matrix $\mathbf{X}$ as X_{ij}. The shorthand $\overline{\mathbf{X}}$ denotes a matrix that its row vectors are normalized and to sum to 1. $\mathbb{I}(\mathbf{X})$ is an indicator function that returns a matrix in the same

a

b
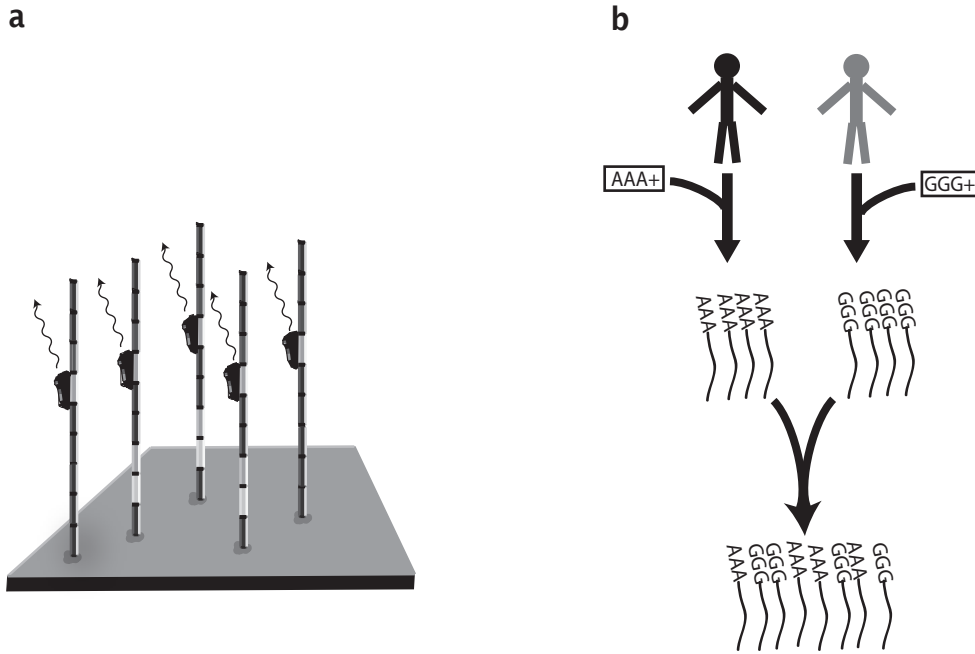
Fig. 1. Common Techniques in Next Generation Sequencing (a) High throughput sequencing is employed by immobilizing DNA fragments (rods) on a slide, and using sequencing reagents (black ovals) that generate optical signals. (b) DNA barcoding is based on synthesizing short DNA sequences, in the example 'AAA' and 'GGG', and ligating them to the samples in distinct reactions. When the samples are mixed the barcodes maintain the identities of the specimens.

size as $\mathbf{X}$ with:

$$\mathbb{I}(X_{ij}) = \begin{cases} 1 & X_{ij} > 0 \\ 0 & X_{ij} = 0 \end{cases}$$

For example:

$$\mathbf{X} = \begin{bmatrix} 0 & 1 \\ 2 & 3 \end{bmatrix}$$

$$\overline{\mathbf{X}} = \begin{bmatrix} 0 & 1 \\ 0.4 & 0.6 \end{bmatrix}$$

$$\mathbf{I}(\mathbf{X}) = \begin{bmatrix} 0 & 1 \\ 1 & 1 \end{bmatrix}$$

The operation $|\cdot|$ denotes the cardinality of a set or the length of a vector. For graphs, ∂a refers to the subset of nodes that are connected to the node a, and the notation $\partial a \backslash b$ means the subset of nodes that are connected to a except of node b. We use natural logarithms.

B. Genotyping As Bipartite Graph Reconstruction

Consider a single human specimen that is being genotyped for a gene that has two alleles, labled by A and a. We represent the genotype of this specimen by a vector of length two with three possible outcomes: $(2, 0)$ if the specimen is homozygous for the A allele, $(1, 1)$ if the specimen is heterozygous, and $(0, 2)$ if the specimen is homozygous for the a allele. This representation can also accommodate situations where the gene has more than two alleles in the population by increasing the length of the vector to the number of the alleles.

The genotype of n individuals is represented by an $n \times s$ matrix $\mathbf{G}$, called the *genotype matrix*, that is composed of the genotype vectors as its rows; G_{ij} denotes how many copies of the j-allele the i-individual holds. For example, consider the follwing genotyping matrix with 6 individuals and only 2 alleles:

$$\mathbf{G} = \begin{bmatrix} 2 & 0 \\ 2 & 0 \\ 2 & 0 \\ 1 & 1 \\ 2 & 0 \\ 0 & 2 \end{bmatrix}$$

In that case, the 4th individual is a carrier, the 6th is affected, and the others are normal.

The genotyping matrix can be represented by a bipartite graph. Let G be a bipartite multigraph, $G = (X, S, E, p)$ that is built according to the genotype matrix, where X is a set of n specimens, S is a set of s possible alleles in the population, and the edge set, E, denotes which subset of alleles each specimen holds. The degree of the specimen nodes, $\deg(x_i)$, is a constant denoted by p, which represents the genome ploidy [1] and in human $p = 2$. The degree of each allele node, $\deg(s_i)$, is a random variable that is dictated by the prevalence of the genotypes in the population. According to that representation, genotyping is in general the task of reconstructing the bipartite

---

[1] this assumption is valid for the vast majority of the genotyping problems, but some particular cases that involve copy number variation, such as Spinal Muscular Atrophy (SMA) [23], do not have a constant degree in their specimen nodes. They will remain outside the scope of this manuscript. In addition, for the sex chromosomes in male $p = 1$.
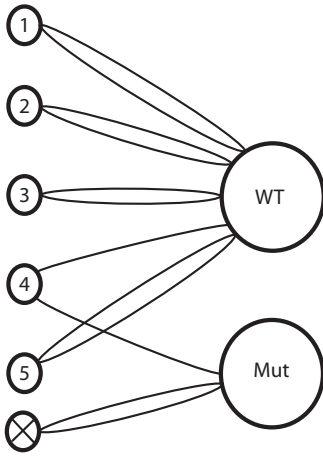
Fig. 2. Cystic Fibrosis $\Delta F508$ Screen as a Bipartite Multigraph Reconstruction. There are two allele nodes, the WT and the $\Delta F508$ mutation. Samples 1, 2, 3, 5 are WT, while specimen 4 is a carrier. The specimen labeled with 'X' is affected and does not enter to the screen. E_{risk} is the edge between specimen 4 and the 'Mut' node.

graph from the sequencing information - finding the edge set E where X and S are known, subject to $p = 2$.

In a carrier screen, one is mainly interested in reconstructing a part of the graph, E_{risk}, that represents the subset of individuals that are carriers of the recessive risk alleles. The graph is very sparse due to the low prevalence of the risk alleles. Moreover, a large portion of severe genetic disease exhibit *complete penetrance* [24], meaning that the affected individuals are symptomatic, and therefore are known, and do not participate in the screen. Thus, finding that one edge of a given individual is connected to a risk allele node immediately implies that the other edge is connected to a non-risk allele node, which further reduces the degrees of freedom in the graph reconstruction.

Consider two examples of carrier screens. First, consider a screen for $\Delta F508$, the most prevalent mutation in Cystic Fibrosis (CF) among people of European descent (Fig. 2). In that case, the set S has two members: WT and mutant, and the expectation of the ratio between $\deg(s_{mutant})$ to $\deg(s_{WT})$ is around 1:29 for screens in European [25] [26]. Most of specimen nodes sends double edges to the WT node, which implies that these specimens carry two copies of the normal allele. A small portion of specimen nodes are connected to the two different allele nodes, meaning that these specimens are carriers for CF. There are no specimens that are connected by double edges to the mutant allele, since this mutation always leads to CF, and the affected individuals do not participate in the screen. Consider also a screen with multiple risk alleles, as in the case of FMR1 gene that causes Fragile X mental retardation [27]. This gene has dozens of alleles, but only a small subset causes the disease. Therefore, we need only to resolve edges to the risk alleles. However, we are intrested in more than a binary classification of the specimens to carriers and normals, as the causative alleles carry different degrees of disease risk (technically known as penetrance), and identifying the exact allele vector has clinical utility.

C. Defining a Cost-effective Reconstruction

Following the analysis above, a genotyping assay is a query of the form: "which allele nodes are connected to the interrogated specimen nodes?". The current DNA sequencing methods that rely on serial specimen processing perform this query for each individual separately. However, the sparsity and the restricted structure of G suggest that E_{risk} may be found in a relatively small number of queries when performing the queries on pools of specimens. Fortunately, the sequencing capacity of next generation sequencers enables the querying of pools of large numbers of specimens.

We will refer to the task of reconstructing G in the most cost effective way as the *minimal genotyping problem*. Note that this task is intentionally not defined as minimizing the number of queries, since there are additional factors that determine the cost and the feasibility of the procedure.

We envision a minimal genotyping strategy that is based on a non-adaptive query schedule in order minimize the turnover time and the need to re-pool the specimens multiple times. Our strategy starts by pooling samples of the specimens according to a certain design as denoted by Φ, which is a $t \times n$ binary matrix; the columns of Φ represent specimens, and each row determines a pool of specimens to be queried. For example, if the first row of Φ is $(1, 0, 1, 0, 1...)$, it specifies that the $1^{st}, 3^{rd}, 5^{th}, ...$ specimens are pooled and queried (sequenced) together. Since the pooling is carried out using a liquid handling robot that can take several specimens in every batch, we only consider designs in which all specimens are sampled the same number of times to reduce the robotic logistics. We define the *weight* w of Φ to be the number of times a specimen is sampled, or the number of 1 entries in a given column vector: every column is constrained to have the same number of 1's in this design. Let r_i be the *compression level* of the i_{th} query, namely the number of 1 entries in the ith row, which denotes the number of specimens in the ith pool.

In large scale carrier screens, n is typically between few thousands to tens of thousands of specimens. We restrict ourself to query designs with $r_{max} \lesssim 1000$ specimens, due to technical / biological limitations (in DNA extraction and PCR amplification) when processing pools with larger number of specimens. A single query in such designs, even when composed of 1000 specimens, does not saturate the sequencing capacity of next generation platforms. In order to fully exploit the capacity, we will pool queries together into *query groups* until the size of each group reaches the sequencing capacity limit, and we will sequence those groups in distinct reactions. Before pooling the queries, we will label each query with a unique DNA barcode in order to retain its identity (for an in-depth protocol of this approach see [20]). Thus, the number of queries, t, is proportional to the number of DNA barcodes that should be synthesized, and one objective of the query design, similar to those found in group testing and compressed sensing, is to minimize t.

In practice, once the DNA barcodes are synthesized, there is enough material for a few dozens experiments, and one can re-use the same barcode reagents for every query group as

TABLE II

SUMMARY OF QUERY DESIGN PARAMETERS

Notation	Meaning	Typical Values	Comments
$\boldsymbol{\Phi}$	Query design		
n	Number of specimens	Thousands	
t	Number of queries (pools)		
w	Weight	$\leqslant 8$	Number of times a specimen is sampled
r_{max}	Max. level of compression	$\lesssim 1000$	Maximal number of specimens in a pool
τ_{max}	Number of queries in the largest query group	Up to a few hundreds	Corresponds to barcode synthesis reactions for a single experiment

these are sequenced in distinct reactions. Hence, the number of queries in the largest pooling group, τ_{max}, dictates the synthesis cost for a small series of experiments. While this does not change the asymptotic cost (e.g. for synthesizing barcodes for a large series of experiments), it has some practical implications, and we will include it in our analysis.

The overall sequencing capacity needed for genotyping is proportional to $\sum_{i=1}^{t} r_i$, the total sum of the sizes of the queries. By definition $nw = \sum_{i=1}^{t} r_i$. Thus, the weight w determines the requisite sequencing capacity for a given number of specimens, and it is an additional factor that should be minimized in order to achieve a cost effective design. Moreover, decreasing the weight also reduces the number of times a specimen is sampled, and consequently, the robot time, and the amount of material that is consumed. Notice that minimizing the weight of the design is not required by traditional compressed sensing construction.

Next generation sequencers are usually composed of several distinct biochemical chambers, called 'lanes', that can be processed in a single batch. We assume that the sequencing capacity needed for n specimens corresponds to one lane[2]. Since in total nw aliquots of specimens are sampled in the pooling step, one needs w lanes to sequence the entire design, where each lane is loaded with a different query group.

We do not intend to specify a global cost function that includes the costs of barcode synthesis, robotic time, sequencing lanes, and other reagents. Clearly, these costs vary with different genotyping strategies, sequencing technologies, and so on. Rather, we will present heuristic rules that would be applicable in most situations. First, w should not exceed the maximal number of lanes that can be processed in a single sequencing batch, as launching a run is expensive and time consuming, and currently, for the most widespread next-generation sequencing platform, $w \leq 8$ [29]. Therefore, it is also desirable that a design construction will have an explicit mechanism to specify the target weight. Second, we assume that the cost of adding a sequencing lane is about two to three orders more than the cost of synthesizing an additional barcode. This will mainly served to benchmark the results of our design to the outcome of other designs that were studied in group testing. Table II presents the notations we used in

[2] recent data have shown that when the number of specimens is a few thousand up to tens of thousands this assumption is valid [28]

that part.

To conclude this part, the query design for the minimal genotyping problem is to find a $t \times n$ design matrix composed of 0's and 1's $\boldsymbol{\Phi}$ that that provides sufficient information to reconstruct G, while minimizing t and keeping the column sum or weight w below a certain threshold. We term a design that addresses these objectives as *light weight design*.

D. The Compositional Channel

The sequencing procedure starts by capturing random DNA molecules from the input material, and therefore, the ratios of sequence types reflect the corresponding ratios of the genotypes in the input material. For example, consider a sample that is composed of a mixture of two specimens in equal ratio, where one specimen is homozygous WT and the other is heterozygous. About $3/4$ of the sequence reads will correspond to the WT allele and $1/4$ to the mutant genotype. Since the input material in our case is composed of pools of specimens, the sequencing results are given by the following conditional probability:

$$f_\beta(\mathbf{Y} \mid \boldsymbol{\Phi}\mathbf{G}) \tag{1}$$

where $\mathbf{Y}$ is a $t \times s$ matrix that denotes the sequencing results, namely the number of sequence reads for each genotype/query combination, and $\mathbf{G}$ is the $n \times s$ biadjacency matrix of the genotyping graph. β is a sampling parameter, a non-negative integer that denotes the number of reads for each query. In reality, β is a random variable with Poisson distribution, since each query has different number of reads. However, for simplicity we will treat it as a constant. $f_\beta(\mathbf{Y} \mid \mathbf{X})$ denotes a multinomial random process that corresponds to the sampling procedure of the sequencers, the joint distribution of the sequencing results is therefore given by

$$f_\beta(\mathbf{Y} \mid \mathbf{X}) = \prod_{i=1}^{t} \alpha_i \exp\left(-\beta \sum_{j=1}^{s} \overline{Y}_{ij} \log(1/\overline{X}_{ij})\right) \tag{2}$$

where $\alpha_i = \frac{\beta!}{\prod_{j=1}^{s} Y_{ij}!}$. As $\beta \to \infty$ the relative ratios of a row in $\mathbf{Y}$ become similar to the ratios of allele nodes degrees of the subgraph induced by the specimens in the pool. We will term the process in Eq. (1) *compositional channel* with parameter β. The reason that we used this name is that the channel places

s-dimensional real space input vectors in an $s-1$-dimensional simplex, which is reminiscent of the concept of compositions in data analysis [30].

The compositional channel is closely related to two other channels, the *superimposed channel*, and the *real adder channel*. As we mentioned earlier, the superimposed channel has been extensively studied in the group testing literature, and describes queries that only return the presence or absence of the tested feature among the members in the pool. On pooled data, measured without noise, the superimposed channel would be given by:

$$\mathbf{Y}_s = \mathbb{I}(\mathbf{\Phi G}) \qquad (3)$$

The information degradation here is more severe than in the case of the compositional channel, since the observer can not quantify the number of positive items from a single query with positive answer. The output of the compositional channel can be further processed as if it was obtained by a superimposed channel. In that case $\mathbf{Y}_s$ denotes only the presence / absence of an allele in a query. This degradation is given by:

$$\mathbf{Y}_s = \mathbb{I}(\mathbf{Y}) \qquad (4)$$

The real adder channel describes the result of a query as a linear combination of the samples in the pool, and is given by:

$$\mathbf{Y}_l = \mathbf{\Phi G} \qquad (5)$$

This type of channel serves as the main model for compressed sensing, and it captures many physical phenomena. A closely related models were studied in group testing for finding counterfeit coins with a precise spring scale [31] and in multi-access communication [32] [33] [34]. Ideally, when one knows the number of specimens in each pool, and $\beta \to \infty$, data from the compositional channel can be treated as if it was obtained by a real adder channel, since the compositional vectors can be placed back in the real space by normalizing $\mathbf{Y}$ to $\overline{\mathbf{Y}}$ and multiplying the result with the number of specimens in each query.

In reality, the sequencer may also produce errors when reading the DNA fragments. Since the fragments are composed of a barcode region and the interrogated region, sequencing errors may lead to association of sequence reads with the wrong query, and to an incorrect genotype detection. DNA barcodes can be easily extended in order to add more redundancy to the codeword that they carry, and experience has demonstrated that that errors in barcode annotation are insignificant [35], and we will not treat this type of errors. On the other hand, sequencing errors in the interrogated region are more involved and we will classify them into two categories according to their outcome: *confounding errors*, meaning that a sequence read that was derived from one genotype is decoded as another valid genotype, and *non-sense errors*, meaning that a decoded sequence read does not correspond to any allele node in G. Non-sense errors are easily handled, for instance, by filtering those sequence reads, as we assume that all possible alleles are known beforehand. Unfortunately, there is no simple remedy for confounding errors, and they may distort the observed allele ratios in the queries. For instance, consider a pool of 100 specimens none of which has a mutant allele that is sampled

TABLE III
Comparison of Different Channels Models

Channel model	Measurement process	Example
Superimposition	OR operation	Antibody reactivity
Compositional	Multinomial sampling	Next generation sequencing
Real Adder	Additive	Spring scale

with $\beta \to \infty$. If the confounding error rate is 0.5%, the data will falsely indicate that one of the specimens in the pool is a carrier. The effect of the sequencing errors on genotyping may be denoted by a conditional probability which includes a confusion matrix:

$$f_\beta(\mathbf{Y} \mid \mathbf{\Phi G \Lambda}) \qquad (6)$$

$\mathbf{\Lambda}$ denotes an $s \times (s+1)$ confusion matrix that indicates the probability that the ith genotype is confounded with the jth genotype; the $s+1$ column indicates the transition probability to a non-sense genotype. We will call the process in Eq. (6) *compositional channel with errors*.

The values of $\mathbf{\Lambda}$ are dependent on the sequence differences between the interrogated alleles and on the specific chemistry that is utilized by the sequencing platform. Based on previous work regarding the most abundant next generation sequencer [28] [36], we presume that subtle mutation differences (known as SNPs), such as $W1282X$ mutation in CF or $Y231X$ mutation in Canavan disease, correspond to confounding error rates of up to 1%, and when the sequence differences are more profound, like in $\Delta F508$ mutation in CF, we expect that the $s \times s$ left submatrix in $\mathbf{\Lambda}$ will resemble the identity matrix. Table III summarizes the different channel models in this section.

III. QUERY DESIGN

A. Constraints On Light-Weight Designs

Group testing theory suggests a sufficient condition for $\mathbf{\Phi}$, called d-disjunction, that ensures faithful and tractable reconstruction of any up to d sparse vector that was obtained from a superimposed channel [12]. Since the compositional channel can be degraded to a superimposed channel, d-disjunction is also a sufficient criterion for reconstructing a d sparse vector over a noise free compositional channel. Respecting a carrier screen and reconstruction E_{risk}, if each risk allele node has less than d edges, d-disjunction is a sufficient condition to reconstruct E_{risk} given a sufficient sequencing depth and no errors.

Based on the analysis about cost effective designs, we are looking for non-trivial d-disjunct matrices that reduce the number of barcodes with a minimal increase of the weight.

Definition 1: $\mathbf{\Phi}$ is called *d-disjunct* if and only if the Boolean sum of up to d column vectors of the matrix does not include any other column vector.

Definition 2: $\mathbf{\Phi}$ is called *reasonable* if it does not contain a row with only a single 1 entry, and its weight is more than 0.

We are only interested in reasonable designs. Clearly, if a design includes queries composed of single specimens, it is

more cost effective to genotype those specimens in serial processing.

Definition 3: λ_{ij} is the dot-product of two column vectors of $\mathbf{\Phi}$, and $\lambda_{\max} \triangleq \max(\lambda_{ij})$.

Lemma 4: The minimal weight of a reasonable d-disjunct matrix is: $w = d + 1$.

Proof: Assume that λ_{max} occurs between $\overrightarrow{C(i)}$ and $\overrightarrow{C(j)}$, two column vectors in $\mathbf{\Phi}$. According to definition (2), every 1 entry in $\overrightarrow{C(i)}$ intersects with at least one column vector. Thus, there are at most w column vectors that intersect with $\overrightarrow{C(i)}$. The Boolean sum of those w column vectors includes $\overrightarrow{C(i)}$, so the matrix is not w-disjunct. According to definition (1), it can not be d-disjunct, and $w \geq d + 1$. The existence d-disjunct matrices with $w = d + 1$ was proved by Kautz and Singleton [12]. ∎

Definition 5: $\mathbf{\Phi}$ is called *light-weight* d-disjunct in case $w = d + 1$.

Lemma 6: $\mathbf{\Phi}$ is a light-weight $(w-1)$-disjunct iff $\lambda_{max} = 1$ and $\mathbf{\Phi}$ is reasonable.

Proof: First we prove that if $\mathbf{\Phi}$ is a light-weight $(w-1)$-disjunct then $\lambda_{max} = 1$. Assume λ_{max} occurs between $\overrightarrow{C(i)}$ and $\overrightarrow{C(j)}$. According to definition (2), there is a subset of at most $w - \lambda_{max} + 1$ column vectors that $\overrightarrow{C(i)}$ is included in their Boolean sum. However, the Boolean sum of any $w - 1$ column vectors does not include $\overrightarrow{C(i)}$. Thus, $\lambda_{max} < 2$, and according to definition (2), $\lambda_{max} > 0$. Thus, $\lambda_{max} = 1$. In the other direction, Kautz and Singelton [12] proved that $d = \lfloor (w-1)/\lambda_{max} \rfloor$, and $\mathbf{\Phi}$ is light-weight according to definition (5). ∎

Lemma 7: The number of columns of $\mathbf{\Phi}$ is bounded by:

$$n \leq \frac{\binom{t}{\lambda_{max}+1}}{\binom{w}{\lambda_{max}+1}} \qquad (7)$$

Proof: see Kautz and Singelton [12]. ∎

Theorem 8: The minimal number of rows, t, in a light-weight d-disjunct matrix is $t > \sqrt{w(w-1)n}$

Proof: plug lemma (6) to lemma (7):

$$n \leq \frac{\binom{t}{2}}{\binom{w}{2}}$$

$$n \leq \frac{t^2}{w(w-1)}$$

$$\sqrt{w(w-1)n} \leq t$$

∎

Corollary 9: The minimal number of barcodes is $\tau_{max} \simeq \sqrt{n}$ in a light-weight weight design.

Proof: There are w query groups, and the bound is immediately derived from theorem (8). ∎

A light weight design is characterized by $\lambda_{max} = 1$, and $t \sim \Omega((d+1)\sqrt{n})$ rows. The low λ_{max} attribute does not only increase the disjunction of the matrix but also eliminates

any short cycle of 4 in the factor graph built upon $\mathbf{\Phi}$, which enhances the convergence of the reconstruction algorithm. We will discuss this property in section IV.

B. Light Chinese Design

We suggest a light weight design construction based on the Chinese Remainder Theorem. This construction reduces the number of queries to the vicinity of the lower bound derived in the previous section, and can be tuned to different weights and numbers of specimens. The repetitive structure of the design simplifies its translation to robotic instructions, and permits easy monitoring.

Constructing $\mathbf{\Phi}$ starts by specifying: (a) the number of specimens, and (b) the required disjunction, which immediately determines the weight. Accordingly, a set of w positive integers $Q = \{q_1, \ldots, q_w\}$, called *query windows*, is chosen with the following requirement:

$$\forall \{q_i, q_j\}, i \neq j : \ lcm(q_i, q_j) \geq n \qquad (8)$$

where lcm denotes the least common multiplier. We map every specimen x to a residue system $(r_1, r_2, \cdots, r_w)$ according to:

$$\begin{aligned} x &\equiv r_1 \pmod{q_1} \\ x &\equiv r_2 \pmod{q_2} \\ &\ \vdots \\ x &\equiv r_w \pmod{q_w} \end{aligned} \qquad (9)$$

Then, we create a set of w all-zero sub-matrices $\mathbf{\Phi}^{(1)}, \mathbf{\Phi}^{(2)}, \cdots$ called *query groups* with sizes $q_i \times n$. The submatrices captures the mapping in Eq. (9) by setting $\mathbf{\Phi}^{(i)}_{rx} = 1$ when this clause: $x \equiv r \pmod{q_i}$ is true. Finally, we vertically concatenate the submatrices to create $\mathbf{\Phi}$:

$$\mathbf{\Phi} = \begin{bmatrix} [\mathbf{\Phi_1}] \\ \hline [\mathbf{\Phi_2}] \\ \hline \vdots \\ \hline [\mathbf{\Phi_w}] \end{bmatrix} \qquad (10)$$

For instance, this is[3] $\mathbf{\Phi}$ for $n = 9$, and $w = 2$, with $\{q_1 = 3, q_2 = 4\}$:

$$\mathbf{\Phi} = \begin{bmatrix} 1 & 0 & 0 & 1 & 0 & 0 & 1 & 0 & 0 \\ 0 & 1 & 0 & 0 & 1 & 0 & 0 & 1 & 0 \\ 0 & 0 & 1 & 0 & 0 & 1 & 0 & 0 & 1 \\ \hline 1 & 0 & 0 & 0 & 1 & 0 & 0 & 0 & 1 \\ 0 & 1 & 0 & 0 & 0 & 1 & 0 & 0 & 0 \\ 0 & 0 & 1 & 0 & 0 & 0 & 1 & 0 & 0 \\ 0 & 0 & 0 & 1 & 0 & 0 & 0 & 1 & 0 \end{bmatrix}$$

Definition 10: Construction of $\mathbf{\Phi}$ according to Eq. (8, 9, 10) is called light Chinese design.

Theorem 11: A light Chinese design is a light weight design.

---

[3] when $x = q_i$ we set $r_i = q_i$, so the first row in every submatrix is 1

Proof: Let $x \equiv v_x \pmod{q_i}$ and $x \equiv u_x \pmod{q_j}$, where $i \neq j$. According to the Chinese Remainder Theorem there is a one-to-one correspondence $\forall x : x \leftrightarrow (u_x, v_x)$. Thus, every two positive entries in $\overrightarrow{C_x}$ are unique. Consequently, $|\overrightarrow{C_x} \cap \overrightarrow{C_y}| < 2$, and $\lambda_{max} < 2$. Since specimens in the form $r, r + q_i, r + 2q_i, \ldots$ are pooled together Φ, $\lambda_{max} = 1$. According to lemma (6) Φ is light-weight. $\blacksquare$

C. Choosing the Query Windows

The set of query windows, Q, determines the number of rows in Φ as:

$$t = \sum_{i=1}^{w} q_i \tag{11}$$

Since $lcm(x,y) = \frac{xy}{gcd(x,y)}$, where gcd is the greatest common divisor, minimizing the elements in Q subject to the constraint in Eq. (8) implies that $q_1, \ldots, q_w$ should be pairwise coprimes and $q_i \geq \sqrt{n}$. Let $\kappa = \lceil \sqrt{n} \rceil - 1$, the definition of the problem we seek to solve is as follows: given a threshold, κ, and w, a valid solution is a set, R, that contains w co-prime numbers, all of which are larger than κ. We seek for the optimal solution, Q, being the solution satisfying that $\sum(Q)$ is minimal.

We begin by introducing a bound on $\max(Q) - \kappa$, a value we will name δ, or the discrepancy of the optimal solution. In order to give an upper bound on δ, let us first consider a bound that is not tight, δ_0, the discrepancy of the solution Q_0 that is composed of the w smallest primes greater than κ. Primes near κ have a density of $1/\log(\kappa)$, so $\delta_0 \approx w \log(\kappa)$. δ_0 is known to be an upper bound on δ because if any value greater than $\kappa + \delta_0$ appears in the Q, then there is also a prime q, $\kappa < q \leq \max(Q_0)$ that is not used. There is at most one value in Q that is not co-prime with q and if it exists it is larger than q. Replace it by q in Q (or replace $\max(Q)$ with q if all numbers in Q are co-prime with q) to reach a better solution, contradicting our assumption that Q is the optimal solution.

This upper bound can improved as follows. We know that $Q \subset (\kappa, \kappa + \delta_0]$. In this interval, there is at most one value that divides any number greater or equal to δ_0. Consider, therefore, the solution Q_1 composed of the w smallest numbers larger than κ that have no factors smaller than δ_0. In order to assess the discrepancy of this solution, δ_1, note that the density of numbers with no factors smaller than δ_0 is at least $1/\log(\delta_0)$. This can be shown by considering the (lower) density that is the density of the numbers with no factors smaller than p_{δ_0}, where p_i indicates the i'th smallest prime. This density is given by:

$$\prod_{i < \delta_0} 1 - \frac{1}{p_i} = e^{\log\left(\prod_{i<\delta_0} 1 - \frac{1}{p_i}\right)}$$
$$= e^{\sum_{i<\delta_0} \log(1 - \frac{1}{p_i})}$$
$$\approx e^{\sum_{i<\delta_0} -\frac{1}{p_i}} \tag{12}$$
$$\approx e^{-\log(\log(\delta_0))}$$
$$= \frac{1}{\log(\delta_0)}$$

where e is Euler's constant and we make use of $\sum_{i<\delta_0} \frac{1}{p_i} \approx \log(\log(\delta_0))$, a well-known property of the prime harmonic series. Like δ_0, the bound δ_1 is also an upper bound on δ. To show this, consider that the optimal solution Q may have z values larger than $\kappa + \delta_1$ in it. If so, there are at least z members of Q_1 absent from it. Replace the z members of Q with the absent members of Q_1 to reach an improved solution. We conclude that $z = 0$ and $\delta_1 \geq \delta$.

Theorem 12: For $\kappa \rightarrow \infty$ and large w, $\delta \approx w \log(w)$.

Proof: Consider repeating a similar improvement procedure as was used to improve from δ_0 to δ_1 an arbitrary number of times. We define Q_{i+1} as the set of w minimal numbers that are greater than κ and have no factors smaller than δ_i, where δ_i is the discrepancy of solution Q_i. This creates a series of upper bounds for δ that is monotone decreasing, and therefore converges. Because each δ_{i+1} satisfies $\delta_{i+1} \approx w \log(\delta_i)$, we conclude that the limit will satisfy $\delta_\infty \approx w \log(\delta_\infty)$, meaning $\delta \leq \delta_\infty \approx w \log(w)$. This gives an upper bound on δ. To prove that this bound is tight, we will show that, asymptotically, it is not possible to fit w co-prime numbers on an interval of size less than $w \log(w)$. To do this, note first that at most one number in the set can be even. Fitting $w - 1$ odd numbers requires an interval of size at least $2w$ (up to a constant). The remaining numbers can contain at most one value that divides by 3. The rest must be either 1 or 2 modulo 3. This indicates that they require an interval of at least $2 \cdot \frac{3}{2} w$. More generally, if S contains w values, with each of the first w prime numbers dividing at most one of said values, then the interval length of S must be at least on the order of:

$$w \prod_{i<w} 1 + \frac{1}{p_i} = w e^{\log\left(\prod_{i<w} 1 + \frac{1}{p_i}\right)}$$
$$= w e^{\sum_{i<w} \log\left(1 + \frac{1}{p_i}\right)}$$
$$\approx w e^{\sum_{i<w} \frac{1}{p_i}}$$
$$\approx w e^{\log(\log(w))}$$
$$= w \log(w)$$

This gives a lower bound on δ equal to the previously calculated upper bound, meaning that both bounds are tight. $\blacksquare$

Corollary 13: $\tau_{max} = \sqrt{n} + w \log(w)$
Proof:

$$\max(Q) - \kappa = \delta$$
$$\max(Q) = \sqrt{n} + \delta$$
$$\max(Q) = \sqrt{n} + w log(w)$$

Since the number of positive entries in each submatrix is the same and equals to n the query groups are formed by partitioning Φ to the submatrices. Consequently, $\tau_{max} = \max(Q)$. $\blacksquare$

Importantly, the maximal compression level, r_{max}, is never more than $\sqrt{n}$, and the light Chinese design is practical for genotyping tens of thousands of specimens. The tight bound on δ also implies a tight bound on the sum of Q. Let

$\sigma_Q = \sum_{i=1}^{w} q_i - w\kappa$. We give a tight bound on $\sigma_Q - w\kappa$ that, asymptotically, reaches a 1:1 ratio with the optimal value.

Theorem 14: The number of queries in the light Chinese design is $t \approx \Theta(w\kappa + \frac{1}{2}w^2 \log(w))$

Proof: Proof that this is a lower bound is by induction on w. Specifically, let us suppose the claim is true for Q_{w-1} and prove for Q_w. (There is no need to verify the "start" of the induction, as any bounded value of w can be said to satisfy the approximation up to an additive error.) To prove a lower bound, σ_{Q_w} cannot be better than $\sigma_{Q_{w-1}} + w\log(w)$, as the discrepancy of Q_w is known and the partial solution $Q_w \setminus \max(Q_w)$ can not be better than Q_{w-1}. To prove that this is also an upper bound, consider that the discrepancy of Q_w is known to be approximately $w\log(w)$, so any prime larger than approximately p_w cannot be a factor of more than one member of the interval $(\kappa, \max(Q_w)]$. Furthermore, the optimal solution for Q_w can not be significantly worse than the optimal solution for Q_{w-1} plus the first number that is greater than $\max(Q_{w-1})$ and has no factors smaller than p_w. As we have shown before, this number is approximately $\max(Q_{w-1}) + \log(w)$. However, we already know the discrepancy of Q_{w-1} is approximately $(w-1)\log(w-1)$, so this new value is approximately $\kappa + (w-1)\log(w-1) + \log(w) \approx \kappa + w\log(w)$. Putting everything together, we get that $\sigma_{Q_w} \leq \sigma_{Q_{w-1}} + w\log(w) \leq \sum_{i \leq w} i\log(i)$, proving the upper bound. The value $\sum_{i \leq w} i\log(i)$ is between $\frac{1}{2}w^2\log(w-1)$ and $\frac{1}{2}w^2\log(w)$, so asymptotically σ_Q converges to $\frac{1}{2}w^2\log(w)$. ∎

We will now consider algorithms to actually find Q. First, consider an algorithm that begins by setting τ_{max} to the w prime number after κ, and then runs an exhaustive search through all sets of size w that contain values between κ and τ_{max}. This is guaranteed to return the optimal result, and does so in complexity $O((\tau - \kappa)^w)$, which is asymptotically equal to $O((w\log(\kappa))^w)$. Though this complexity is hyper exponential, and so unsuitable for large values of w it may be used for smaller w.

The upper bound described above suggests a polynomial algorithm for Q since it is a bound that utilizes sets chosen such that none of their elements have prime factors smaller than κ. This implies the following simplistic algorithm that calculates a solution that is asymptotically guaranteed to have a 1:1 ratio with the optimal σ_Q.

1: Let Q be the set of the w smallest primes greater than κ.

2: **repeat**
3:    $\delta \leftarrow \max(Q) - \kappa$
4:    $Q \leftarrow$ the w smallest numbers greater than κ that have no factors smaller than δ
5: **until** $\delta = \max(Q) - \kappa$
6: output Q.

In practice, this is never the optimal solution, as for example, it contains no even numbers. In order to increase the probability that we reach the optimal solution (or almost the optimal solution), we opt for a greedy version of this algorithm. The greedy algorithm begins by producing the set of smallest numbers greater than κ that have no factors smaller

than δ (as in the upper bound). It continues by producing the set of smallest co-prime numbers greater than κ that have at most one distinct factor smaller than δ (as in the calculation of the lower bound). Then, it attempts to add further elements with a gradually increasing number of factors. If these attempts cause a decrease in δ, it repeats the process with a lower value of δ until reaching stabilization.

1: $Q \leftarrow$ initial solution.
2: **repeat**
3:    $\delta \leftarrow \max(Q) - \kappa$
4:    $n(x) \overset{\text{def}}{=}$ the number of distinct primes smaller than δ in the factorization of x.
5:    Sort the numbers $\kappa+1, \ldots, \max(Q)$ by increasing $n(x)$ [major key] and increasing value [minor key].
6:    **for all** i in the sorted list **do**
7:        **if** i is co-prime to all members of Q and $i < \max(Q)$ **then**
8:            replace $\max(Q)$ by i in Q.
9:        **else if** i is co-prime to all members of Q except one, q, and $i < q$ **then**
10:            replace q with i in Q.
11:       **end if**
12:   **end for**
13: **until** $\delta = \max(Q) - \kappa$
14: output Q.

Because this greedy algorithm only improves the solution from iteration to iteration, using the output of the first algorithm described as the initial solution for it guarantees that the output will have all asymptotic optimality properties proved above. In practice, on the range $\kappa = 100 \ldots 299$ and $w = 2 \ldots 8$ it gives the exact optimal answer in 91% of the cases and an answer that is off by at most 2 in 96% of the cases. (Understandably, no answer is off by exactly 1.) The worst results for it appear in $w = 8$, where only 82% of the cases were optimal and 88% of the cases were off by at most 2.

Notably, due to the fact that $\kappa + 1$ does not always appear in either the optimal solution or the solution returned by the greedy algorithm, sub-optimal results tend to appear in *streaks*: a sub-optimal result on a particular κ value increases the probability of a sub-optimal result on $\kappa+1$ (A similar property also appears when increasing w), and we denote an interval of consecutive κ values where the greedy algorithm returns sub-optimal results to be a "streak". The number of streaks is, perhaps, a better indication for the quality of the algorithm than the total number of errors. For the parameter range tested (totaling 1400 cases), the greedy algorithm produced 61 sub-optimal streaks (of which in only 23 streaks the divergence from the optimal was by more than 2). The worst w was 6, measuring 14 streaks. The worst-case for divergence by more than 2 was $w = 8$, with 8 streaks.

In terms of the time complexity of this solution, this can be bounded as follows. First, we assume that the values in the relevant range have been factored in advance, so this does not contribute to the running time of the algorithm. (This factorization is independent of κ and w, except in the very weak sense that κ and w determine what the "relevant" range

to factor is.) Next, we note that the initial δ is determined by searching for w primes, so we begin with a δ value on the order of $w \ln(\kappa)$. Each iteration decreases δ, so there are at most $w \log(\kappa)$ iterations. In each iteration, the majority of time is spent on sorting δ numbers. Hence, the running time of the algorithm is bounded by $\delta^2 \log(\delta)$ or $w^2 \log^2(\delta)(\log(w) + \log(\log(\kappa)))$. Clearly, this is a polynomial solution. In practice, it converges in only a few iterations, not requiring the full δ potential iterations. In fact, in the tested parameter range the algorithm never required more than three iterations in any loop, and usually less. (Two iterations in the greedy allocation loop is the minimum possible, and an extra iteration over that was required in only 4% of the cases.)

In some cases, it is beneficial to increase the number of barcodes from κ to κ_1 in order to achieve higher probability of faithful reconstruction of signals that are not d sparse. This is achieved by finding w integers in the interval (κ, κ_1) that follow Eq. (8) and maximize $\prod_{i=1}^{w} q_i$. We give more details about this problem in appendix I.

Lastly, we note that even though these approximation algorithms are necessary for large values of w, for small w an exhaustive search for the exact optimal solution is not prohibitive, even though the complexity of such a solution is exponential. One can denote the solution as $Q = \{\kappa + s_1, \kappa + s_2, \ldots, \kappa + s_w\}$ in which case the values $\{s_1, \ldots, s_w\}$ are only dependent on the value of κ modulo primes that are smaller than the maximal δ or approximately $w \log(w)$. This means that the $\{s_1, \ldots, s_w\}$ values in the optimal solution for any (κ, w) pair is equal to their values for $(\kappa \mod P, w)$, where P is the product of all primes smaller than δ. Essentially, there are only P potential values of κ that need to be considered. All others are equivalent to them.

In practice, the number of different κ values that need to be considered is significantly smaller than this. As an example, Fig. 3 gives the complete optimal solution for any value of κ with $w = 4$. The figure shows that the set $S = \{s_1, \ldots, s_w\}$ for any κ has only 7 possible values, and that determining which set produces the optimal solution for any particular value of κ can be done by at most 5 Boolean queries regarding the value of κ modulo specific primes.

D. Comparison to Logarithmic Designs

It is well established in group testing theory and in compressed sensing that certain designs can reach to the vicinity of the lower theoretical bound of $t \sim O(d \log n)$ [37], [38]. The $t \sim O((d+1)\sqrt{n})$ scale in light weight designs raises the question whether they are really the most cost effective solution for the minimal genotyping problem with thousands of specimens and $w \leqslant 8$.

We compared the results of the light Chinese design with the method of Eppstein and colleagues [39] for screens with 5000 and 40000 specimens (Table IV). To the best of our knowledge, Eppstein's method shows for the general case the maximal reduction of t. Interestingly, it is also based on the Chinese Remainder Theorem, but without the assertion in Eq. (8). Instead, their method requires that Q will be composed of co-prime numbers whose product is more than n^d in order
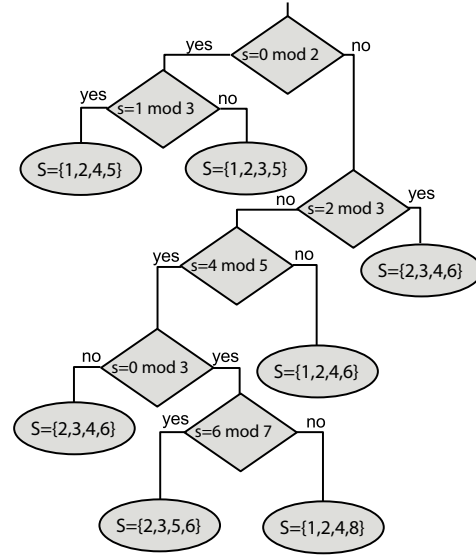
Fig. 3. Optimal Solution using Tree Search

TABLE IV

COMPARISON BETWEEN EPPSTEIN'S METHOD TO THE LIGHT CHINESE DESIGN

n	d	Eppstein				Light Chinese design			
		t	w	τ_{max}	r_{max}	t	w	τ_{max}	r_{max}
5000	3	149	$10^{\dagger}$	29	1000	293	4	77	64
	4	237	$12^{\dagger}$	37	714	370	5	77	64
	5	336	$15^{\dagger}$	47	1000	449	6	79	64
40000	3	209	$12^{\dagger}$	37	$8000^{\dagger}$	811	4	205	199
	4	335	$14^{\dagger}$	47	$5714^{\dagger}$	1020	5	209	199
	5	472	$17^{\dagger}$	59	$5714^{\dagger}$	1231	6	211	199

to create a d-disjunct matrix. The number of queries in their method for a given d is:

$$t \sim O(d^2 \log^2 n/(\log d + \log \log n)) \tag{13}$$

and the weight is:

$$w \sim O(d \log n/(\log d + \log \log n)) \tag{14}$$

Notice that their weight scales with the number of specimens, implying that more sequencing lanes and robotic logistic are required with the growth of n even if d is constant.

First, we found that Eppstein's method is not applicable to the biological and technical constraints in the genotyping setting of $w \leqslant 8$ and $r_{max} \lesssim 1000$ (labeled in the table with $\dagger$). Second, the differences between the number of barcodes, τ_{max}, and the number of queries in their method are no more than ten fold, but their weights are least 2.5 fold greater than the weights in the light Chinese design. With the estimated cost ratio between barcode to sequencing lane to be around $1 : 100$, the light Chinese design is more cost effective. Finally, there is no intrinsic mechanism in Eppstein's method to specify the weight, and to limit it below a threshold.

IV. RECONSTRUCTION ALGORITHMS

A. Bayesian Decoding Using Belief Propagation

Now, we will turn to address the other part of the minimal genotyping problem, which is how to reconstruct $\mathbf{G}$ given $\mathbf{Y}$ and $\mathbf{\Phi}$. In general, this is an ill-posed inverse problem, but the sparsity of $\mathbf{G}$ due to the biological constraints (e.g the diploidy of the genome and the absence of affected individuals in the screen) and the low abundance of rare risk alleles permits such decoding. The MAP decoding of the genotyping problem is given by:

$$\mathbf{G}_{MAP} \triangleq \underset{x_1,\dots,x_n}{\mathrm{argmax}}\, \Pr(x_1,\dots,x_n \mid \mathbf{Y}) \qquad (15)$$

For simplicity, we assume that we do not have any prior knowledge on the specimens, beside the expected frequency of the genotypes in the screen. Notice that kinship information between the specimens and familial history regarding genetic diseases are known is some cases and may enhance the decoding results, however, they will remain outside the scope of this manuscript. η is a probability vector with length of $s(s+1)/2$ that denotes the expected prevalence of each genotype. For instance, for $\Delta F508$ screen $\eta = (29/30, 1/30, 0)$ for normal, carriers, and affected, correspondingly. Let x_i be an instance of row vector in $\mathbf{G}$, and $c(x_i)$ be a binary vector with length as η that maps the allelic configuration of x_i to an entry in a list of genotypes. For instance, if there are two alleles in the population, x_i is either $(2,0)$, $(1,1)$, or $(0,2)$, and $c(x_i)$ is $(1,0,0)$, $(0,1,0)$, or $(0,0,1)$, correspondingly. We denote the prior probability of x_i by:

$$\varphi(x_i) = \prod_{j=1}^{s(s+1)/2} \eta_j^{c_j(x_i)} \qquad (16)$$

The prior probability for a certain graph configuration, $(x_1,\dots,x_n)$, is:

$$\prod_{i=1}^{n} \varphi(x_i) \qquad (17)$$

The data is also a subject to factorization, since the result of a particular query is solely determined by the specimens in the pool:

$$\Pr(\mathbf{Y} \mid x_1,\dots,x_n) = \prod_{a=1}^{t} \Pr(\mathbf{Y}_a \mid x_{\partial a}) \qquad (18)$$

we used $x_{\partial a}$ to denote a configuration of the subset of specimens in the a query, and $\mathbf{Y}_a$ denotes the ath row vector in $\mathbf{Y}$. The probability distribution $\Pr(\mathbf{Y}_a \mid x_{\partial a})$ is given by the compositional channel model in Eq. (6) and since we assume that β and Λ are constant for all the queries, we will use the following shorthand to denote this probability distribution:

$$\Psi_a(x_{\partial a}) \triangleq f_\beta(x_{\partial a}\Lambda) \qquad (19)$$

From Eq. (15-19), we get:

$$\Pr(\mathbf{G}) \propto \prod_{a=1}^{t} \Psi_a(x_{\partial a}) \prod_{i=1}^{n} \varphi(x_i) \qquad (20)$$

The factorization above is captured by factor graph with two types of factor nodes, φ nodes and Ψ nodes. The φ nodes
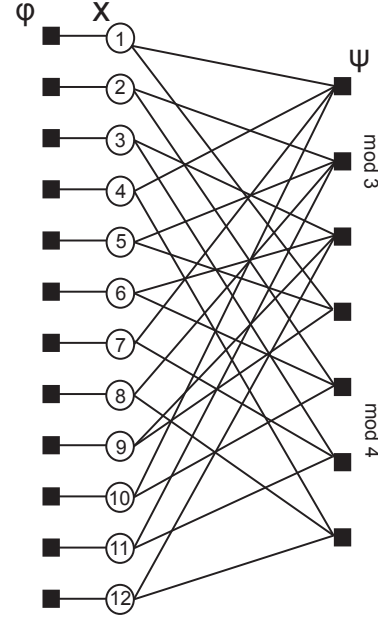
Fig. 4.   Example of Factor Graph for Genotyping Reconstruction

are uniquely connected to each variable nodes, whereas the Ψ nodes are connected to the variables according to the query design in $\mathbf{\Phi}$, so each variable node is connected to w different Ψ nodes. An example of a factor graph with 12 specimens, and $Q = \{3,4\}$ is given in Fig. 4.

Belief propagation (sum-product algorithm) [40], [41] is a graphical inference technique that is based on exchanging messages (beliefs) between factor nodes and variable nodes that tune the marginals of the variable nodes to the observed data. When a factor graph is a tree the obtained marginals are exact; however, a factor graph that is built according to any reasonable query design will always contain many loops (easily proved by the pigeonhole principle), implying that finding G_{MAP} is NP-hard [42]. Surprisingly, it has been found that belief propagation can still be used as an approximation method for factor graphs with loops. These findings rely on the concept that if the local topology of a factor graph is a tree-like, the algorithm can still converge with high probability [43], [44]. This approach has been successfully used in a broad spectrum of NP-hard problems including decoding LDPC codes [40], finding assignments in random k-SAT problems [45] and even solving Sudoku puzzles [46]. Recently, Mezard and colleagues studied the decoding performance of belief propagation in the prototypical problem of group testing [47]. One advantage of their setting is the presence of 'sure zeros' - variables nodes that are connected to at least one 'inactive' test node. Since the tests are faultless in the prototypical problem, those variables are immediately decoded as 'inactive', and are stripped off from the factor graph, which reduces the complexity of problem handed to the belief propagation. Unfortunately, the query results from next generation sequencers are not reliable, and the absence of an allele node from a query may stem from insufficient sequencing coverage (small β) and sequencing errors. Furthermore, the total number of sure zeros

can be very small as confounding errors may falsely indicate the presence of an allele in a query. From these two reasons, stripping has little applicability in our setting. On the other hand, Baron and colleagues [48] investigated the performance of belief propagation for the recovery of compressed signals with a linear channel model and additive white Gaussian noise (AWGN). Our approach is reminiscent of their method, and employs belief propagation on the full graph using some essential shortcuts.

The marginal probability of x_i is given by the Markov property of the factor graph:

$$\Pr(x_i) \propto \varphi(x_i) \prod_{a=1}^{w} \mu_{a \to x_i}(x_i) \qquad (21)$$

The approximation made by belief propagation in loopy graphs is that the beliefs of the variables in the subset $\partial a \backslash x_i$ regarding x_i are independent. Since $\lambda_{max} = 1$ in light-weight designs, the resulted factor graph does not have any short cycles of girth 4, implying that the beliefs does not strongly correlated, and that the assumption is approximately fullfilled. The algorithm defines $\mu_{a \to x_i}(x_i)$ as:

$$\mu_{a \to x_i}(x_i) = \sum_{\{x \in \partial a \backslash x_i\}} \Psi_a(x_{\partial a}) \prod_{x_j \in \partial a \backslash x_i} \mu_{x_j \to a}(x_j) \qquad (22)$$

and

$$\mu_{x_j \to a}(x_j) = \varphi(x_j) \prod_{u \in \partial x_j \backslash a} \mu_{u \to x_j}(x_j) \qquad (23)$$

were $u \in \partial x_j$ denotes the subset of queries with x_j. Eq. (22) describes message from a factor node to a variable node, and Eq. (23) describes message from a variable node to a factor node. By iterating between the messages the marginals of the variable nodes are gradually obtained, and in case of successful decoding the algorithm reaches to a stable point, and reports G^*:

$$G^* \triangleq \underset{x_i}{\operatorname{argmax}} \Pr(x_i) \qquad (24)$$

This approach encouters a major obstacle - calculating the factor to node messages requires summing over all possible genotype configurations in the pool, which exponentially grows with the compression level, r_{max}, or $\sqrt{n}$. To circumvent that, we use Monte-Carlo sampling instead of an exact calculation to find the factor to node messages of each round. This is based on drawing random configurations of $x_{\partial a}$ according to the probability density functions (pdf) that are given by the $\mu_{x_j \to a}(x_j)$ messages and evaluating $\Psi_a(x_{\partial a})$. An additional complication are strong oscillations in which the marginal estimation of x_i for the τ step is almost completely concentrated in one state, but at the $\tau + 1$ step, the estimation is completely concentrated in another state. One of those states is obviously wrong, and a sampling process that uses this pdf to evaluate a factor to node message for other variable nodes may find only very small values of Ψ, which is prone to numerical stability issues that ended up in sending all-zero messages and failure of the algorithm. We used message damping to attenuate the oscillations [49]. The

damping procedure averages the variable to factor messages of the m round with the message of the $m-1$ round:

$$\mu_{x_j \to a}^{m(damped)}(x_j) = \left(\mu_{x_j \to a}^m(x_j)\right)^{1-\gamma} \left(\mu_{x_j \to a}^{m-1}(x_j)\right)^{\gamma} \qquad (25)$$

The extent of the damping can by tuned with $\gamma \in [0, 1]$. When $\gamma = 1$ there are no updated at all, and when $\gamma = 0$ we restore the algorithm in Eq. (23). Appendix II presents a full layout of the belief propagation reconstruction algorithm:

B. Baseline Reconstruction Algorithm

In order to benchmark the belief propagation decoding algorithm above, we introduce an additional algorithm, named *pattern consistency decoding*, which is used in group testing to reconstruct the original data from superimposed channel. In a carrier screen, the algorithm first creates a new matrix that is composed of the columns in $\mathbf{Y}$ that correspond to the risk alleles, and then it treats the results in the new matrix as superimposition according to Eq. (4). We denote the new matrix by $\mathbf{Y}_{rs}$.

This method does not address query errors, and a specimen is defined as a carrier only if all its w queries indicate the presence of a risk allele:

$$\widehat{\mathbf{E}_{risk}} = \mathbb{I}(\mathbf{Y}_s^T \boldsymbol{\Phi}) \qquad (26)$$

where $\mathbb{I}$ is an indicator function:

$$\mathbb{I}(X_{ij}) = \begin{cases} 1 & X_{ij} = w \\ 0 & otherwise \end{cases} . \qquad (27)$$

Rows of E_{risk} with positive entries indicate carriers. This reconstruction is guaranteed to be correct if d_0, the maximal number of carriers in the screen for one of the risk alleles, is lower than d, the disjunction property of $\boldsymbol{\Phi}$, (given no sequencing errors and sufficient coverage). Since this reconstruction works with degraded information compared to belief propagation, we will use it to indicate the baseline performance expected from belief propagation decoding, and to test whether the approximations we employed (loopy messages, Monte-Carlo sampling, damping) are valid.

V. NUMERICAL RESULTS

To demonstrate the power of our method, we simulated several settings where there is one risk allele and one WT allele in the population, with $n = 1000$, $\beta = 10^3$, $w = 5$, and $Q = \{33, 34, 35, 37, 41\}$, which can be accommodated in a single machine batch. Fig. 5 emphasizes the effect of damping on the belief propagation convergence rates. In this example, the number of carriers in the screen was $d_0 = 43$, and we ran the decoder for 30 iterations. We evaluated different extents of damping: $\gamma \in [0.1, \ldots, 0.9]$, and we measured for each iteration the averaged absolute difference in the marginal from the previous step. We found that with $\gamma < 0.5$, there are strong oscillations and the algorithm does not converge, whereas with $\gamma \geqslant 0.5$, there are no oscillations, and the algorithm converges and correctly decodes the genotype for all the specimens.

We also tested the performance of the reconstruction algorithms for increasing number of carriers in the screen,
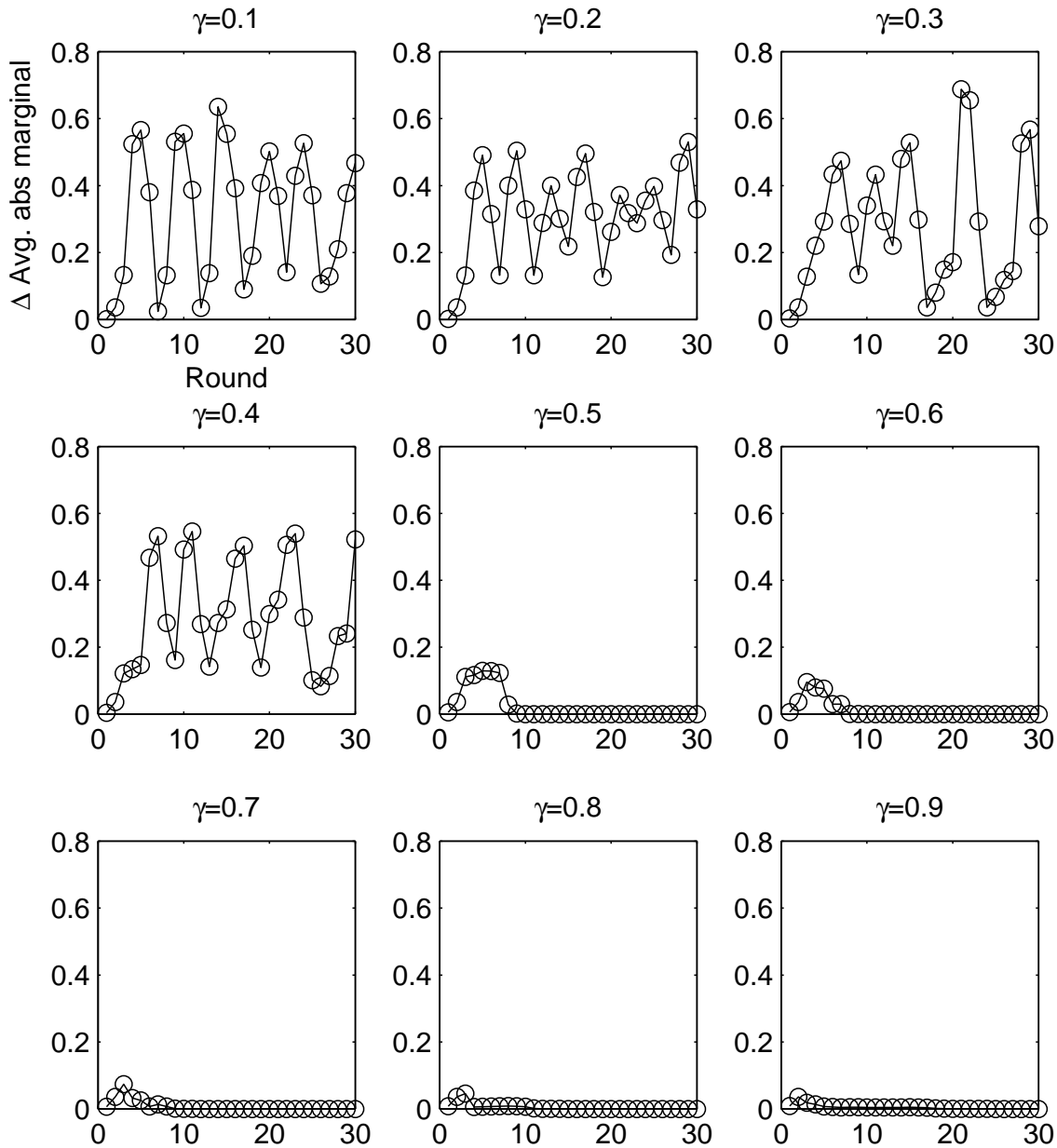
Fig. 5.   The Effect of Damping on Oscillations

ranging from 5 to 150, with no sequencing errors (Fig. 6). The belief propagation reconstruction outperformed the pattern consistency decoder and reconstructed the genotypes with no error even when the number of carriers was 40, which is a quite high number for severe genetic diseases. The ability of the belief propagation to faithfully reconstruct cases with $d_0 \gg d$-disjunction of the query design is not suprising, since d-disjunction is a conservative sufficient condition even for a superimposed channel.

We continue to evaluate the performance of the algorithm in a biologically-oriented setting - detecting carriers for CF $W1282X$ mutation, where the carrier rate in some populations is about 1.8% [26]. The relatively high rate of the carriers challenges our scheme with a difficult genetic screening problem. Moreover, the sequence difference between the WT allele and the mutant allele is only a single base substitution, and sequencing error may cause genotype confounding. To recapitulate that, we introduced increasing levels of symmetric confounding errors (i.e the two alleles have the same probability of being converted from one to the other), and we tested the performance of the reconstruction algorithms with $\beta = 10^3$ and $\beta = 10^4$, and with error rates in the range of $0\% - 4.5\%$ with steps of 0.5% (Fig. 7).

As expected, the pattern consistency decoder performed poorly (data not shown) even for the lowest error rate of 0.5% and marked all specimens as carriers. The belief propagation algorithm reported the correct genotype for all specimens even when the error rate was 1.5% and $\beta = 10^3$. Importantly, the decoding mistakes of the belief propagation at higher error rates were false positives, and did not affect the sensitivity of
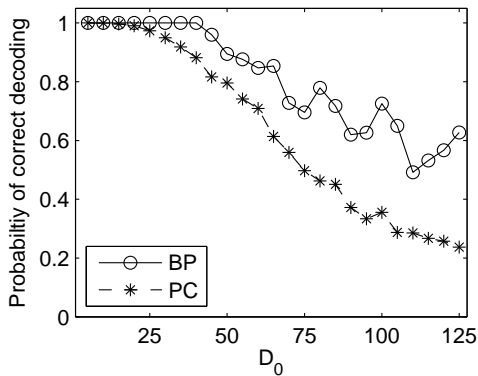
Fig. 6. Decodability as a Function of Number of Carriers
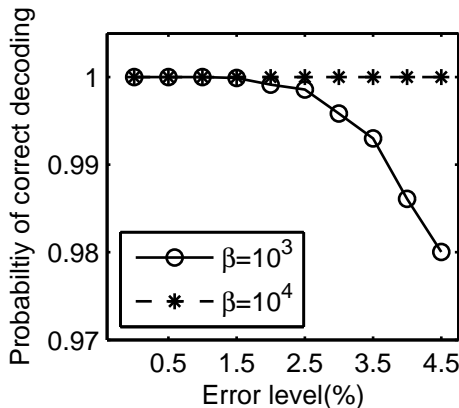
Fig. 7. Simulation of CF Screen - The Effect of β and Confounding Errors
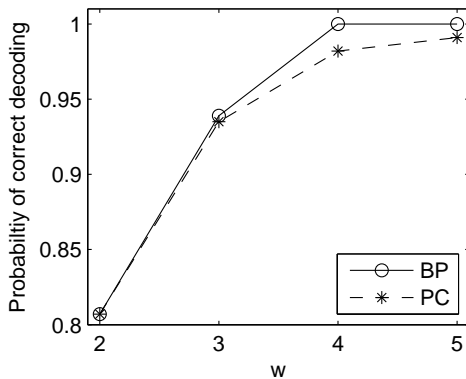
Fig. 8. Different Weights for CF $\Delta F508$ Screen Detection

the method. When we increased the number of reads for each query to $\beta = 10^4$, the belief propagation decoder reported the genotype of all the specimens without any mistake. As we mentioned earlier, the expected confounding error rate for this mutation up to 1%, implying that the parameters used in the simulation are quite conservative.

We also tested another CF mutation, $\Delta F508$, which has a similar carrier rate in people with European descents as $W1282X$, but contains a 3-nucleotide deletion when compared to the WT allele. This implies that the confounding error rates are negligible, as sequencing-induced deletions are

quite rare. In this example, we evaluated the effect of different weights for the query designs, and we used the following sets of query windows: $\{33, 34\}$, $\{33, 34, 35\}$, $\{33, 34, 35, 37\}$, $\{33, 34, 35, 37, 41\}$. Fig. 8 depicts the results for the belief propagation algorithm and for the pattern consistency decoder. While the results are quite poor for $w = 2$, the belief propagation decodes correctly all the specimens with $w = 4$, which would requires the synthesis of only 37 barcodes, and a total of 139 queries.

VI. CONCLUSION

In this paper, we presented a compressed genotyping framework that harnesses next generation sequencers for large scale genotyping screens of severe genetic diseases. We formulated the problem as reconstructing a spares bipartite multigraph from information that was obtained over a compositional channel. In addition to the traditional objective of minimizing the number of queries, we introduced another objective of reducing the weight of the design, and we propose a new class of designs called light-weight designs in which the weight does not depend on n, and only grows linearly with d. For the genotyping reconstruction part, we presented a Baysian framework that is based on loopy belief propagation, and we evaluated its performance by simulating different types of carrier tests, including prevalent mutations in Cystic Fibrosis.

Further investigation is needed to expand the framework to include prior biological data such as familial information and other predispositions, and to include more types of errors beyond those introduced by sequencing, such as biased PCR amplification, query failures, and sample contamination. In addition it will be interesting to develop a more comprehensive treatment for the compositional channel, and to find a less conservative sufficient condition for faithful signal reconstruction.

APPENDIX I
THE PRODUCT MAXIMIZATION ALGORITHM

The product maximization problem is defined as follows. Given parameters κ, κ_1 and w, find the set Q of size w whose elements are all in the range $\kappa < x \leq \kappa_1$ and such that for no pair $x, y \in Q$ has $lcm(x, y) \leq \kappa^2$. For product maximization, typical values in practice have κ in the range $[100, 300)$, w in the range $[2, 8]$ and κ_1 fixed at 384. The reason for this number is the number of wells in a microtiter plate, which is compatible with liquid handling robots. The empirical results below relate to this entire range, for all of which we have optimal solutions discovered by exhaustive searching.

The product maximization problem has ties to the sum minimization problem in both bound-calculation and solving algorithms. First, note that in this problem we cannot consider "asymptotic" behavior when w, κ and κ_1 are large without specifying how the ratio $\frac{\kappa_1}{\kappa}$ is constrained.

If κ is constant and κ_1 rises, the asymptotic solution will be the set $\{\kappa_1, \kappa_1 - 1, \kappa_1 - 2, \ldots, \kappa_1 + 1 - w\}$. This set clearly has the maximum possible product, while at the same time satisfying the condition on the lcm because no two elements in the solution can have a mutual factor greater than w. This value will be the optimum as soon as $(\kappa_1 + 1 - w)(\kappa_1 + 2 - w) > w\kappa^2$

(and possibly even before), so $\sqrt{w}$ should be taken as an upper bound for $\frac{\kappa_1}{\kappa}$ to form a non-trivial case.

For any specific ratio $\frac{\kappa_1}{\kappa}$, the condition $lcm(x,y) > \kappa^2$ for x and y values close to κ_1 is equivalent to $gcd(x,y) < \frac{\kappa_1^2}{\kappa^2}$. This allows us to reformulate the question as that of finding the set Q with w elements, all less than or equal to κ, s.t. the gcd of any pair is lower than or equal to $\rho = \left\lfloor \frac{\kappa_1^2}{\kappa^2} \right\rfloor$.

For the product maximization problem, we redefine the discrepancy to be $\delta = \kappa_1 + 1 - \min(Q)$. In order to compute the asymptotic bound for this discrepancy, let us first define *pseudo-primes*. Let the set of k-pseudo-primes, P_k, be defined as the set s.t. $i \in P_k \iff i > k$ and $\neg\exists j < i, j \in P_k$ s.t. i is divisible by j. The set of 1-pseudo-primes coincides with the set of primes.

One interesting property of k-pseudo-primes is that they coincide with the set of primes for any element larger than k^2. To prove this, first note that if i is a prime and $i > k$ then i by definition belongs to P_k. Second, note that if i is composite and $i > k^2$ then i has at least one divisor larger than k. In particular, it must have a smallest divisor larger than k, and this divisor cannot have any divisors larger than k, meaning that it must belong to P_k. Consequently, $i \notin P_k$.

Both the reasoning yielding the upper bound and the reasoning yielding the lower bound for the sum minimization problem utilize estimates for the density of numbers not divisible by a prime smaller than some d. In order to fit this to the product maximization problem, where a gcd of ρ is allowed, we must revise these to estimates for the density of numbers not divisible by a ρ-pseudo-prime smaller than δ. Because the k-pseudo-primes and the primes coincide beginning with k^2, this density is the same up to an easy-to-calculate multiplicative constant γ_k.

Knowing this, both upper and lower bound calculations can be applied to show that the asymptotic discrepancy of the optimal solution is on the order of $\gamma_k w \ln(w)$. This discrepancy can be used, as before, to predict an approximate optimal product. However, the bound on the product is much less informative than the bound on the sum: the product can be bounded from above by κ_1^w and from below by $(\kappa_1 - \delta)^w$, both converging to a ratio of 1:1 at κ_1 rises.

The revised greedy algorithm for this problem is given explicitly below.

1: Let Q be the set of the w largest primes $\leq \kappa_1$.
2: **repeat**
3:    $\delta \leftarrow \kappa_1 + 1 - \min(Q)$
4:    $Q \leftarrow$ the w largest numbers $\leq \kappa_1$ that have no factors smaller than δ
5: **until** $\delta = \kappa_1 + 1 - \min(Q)$
6: **repeat**
7:    $\delta \leftarrow \kappa_1 + 1 - \min(Q)$
8:    $n(x) \overset{\text{def}}{=}$ the number of distinct primes smaller than δ in the factorization of x.
9:    Sort the numbers $\min(Q), \ldots, \kappa_1$ by increasing $n(x)$ [major key] and decreasing value [minor key].
10:    **for all** i in the sorted list **do**
11:       **if** $\forall q \in Q, lcm(q,i) > \kappa^2$ and $i > \min(Q)$ **then**
12:          replace $\min(Q)$ by i in Q.
13:       **else if** There is exactly one $q \in Q$ s.t. $lcm(q,i) \leq \kappa^2$, and $i > q$ **then**
14:          replace q with i in Q.
15:       **end if**
16:    **end for**
17: **until** $\delta = \kappa_1 + 1 - \min(Q)$
18: output Q.

Note that the greedy algorithm tries to lower the discrepancy of the solution even when there is no proof that a smaller discrepancy will yield an improved solution set. In the sum minimization problem, any change of Δ in any of the variables yields a change of Δ in the solution, so there is little reason to favor reducing the largest element of Q (and thereby reducing the discrepancy) over reducing any other element of Q. In product maximization, however, a change of Δ to $\min(Q)$ (and hence to the discrepancy) corresponds to a larger change to the product than a change of Δ to any other member of Q. This makes the greedy algorithm even more suited for the product maximization problem than for sum minimization.

Indeed, when examining the results of the greedy algorithm on $\kappa = 384$, with $w \in [2, 8]$ and $\kappa \in [100, 300)$ we see that the greedy algorithm produces the correct result in all cases $w \in [2, 3, 4]$. In $w \in [6, 7, 8]$ the algorithm produces the optimal result in all but 2,3 and 3 cases, respectively. The only w for which a large number of sub-optimal results was recorded is $w = 5$ where the number of sub-optimal results was 49. Note, however, that in product maximization there is a much larger tendency for "streaking". The 49 sub-optimal results all belong to a single streak, where the optimal answer is $\{379, 380, 381, 382, 383\}$ and the answer returned from the greedy algorithm is $\{377, 379, 382, 383, 384\}$. The difference in the two products is approximately 0.008%.

In terms of streaks, the optimal answer was returned in all but one streak in $w \in [5, 6]$ and in all but two streaks in $w \in [7, 8]$. In terms of the number of iterations required, the only extra iterations that were needed in the execution of the algorithm beyond the minimal required was a single extra iteration through the first "repeat" loop when w was 3. In all other cases, no extra iterations were used, demonstrating that this algorithm is in practice faster than is predicted by its (already low-degree polynomial) time complexity.

APPENDIX II
FULL LAYOUT OF BELIEF PROPAGATION RECONSTRUCTION

1) **Inputs:** Query design $\mathbf{\Phi}$, sequencing results $\mathbf{Y}$, prior expectations about the genotypes prevalence η, damping parameter γ, number of iterations m_{max}, and number of Monte Carlo rounds z.

2) **Preprocessing:** (a) find β - enumerate the number of reads in the query. (b) learn the genotype error pattern Λ - the sequencing errors rates are estimated using spiked-in controls [36], and converted to genotype error according to the sequence of the different alleles. (c) calculate φ according to η.

3) **Initialization** Initialize the iteration counter m. Initialize $\mu_{x_i \to a}(x_i)$ to priors in φ.

4) **Send messages from factors to variables:**

  1: **for** each factor a in $\{1, \ldots, t\}$ **do**
  2:    **for** each variable x_i in query a **do**
  3:      **for** each state of variable x_i in $\{1, \ldots, |\eta|\}$ **do**
  4:        Set $\Psi_0 \leftarrow 0$
  5:        **for** $\{1, \ldots, z\}$ Monte-Carlo round **do**
  6:          $r \leftarrow$ random configuration of $\partial a \backslash x$ according to pdfs in $\mu^m_{x_j \to a}$
  7:          $\Psi_0 \leftarrow \Psi_0 + \Psi_a(r, \text{state of } x_i)$
  8:        **end for**
  9:        $\mu_{a \to x_i}(\text{state of } x_i) \leftarrow \Psi_0/m$
 10:      **end for**
 11:      Normalize $\mu_{a \to x_i}(x_i)$
 12:      Send message $\mu_{a \to x_i}(x_i)$
 13:    **end for**
 14: **end for**

5) **Send messages from variables to factors:**

  1: **for** each variable x_i in $\{1, \ldots, n\}$ **do**
  2:    **for** each factor a connected to x_i **do**
  3:      Set $\mu^m_{x_i \to a}(x_i)$ to all ones vector.
  4:      **for** each possible state of variable x_i in $\{1, \ldots, |\eta|\}$ **do**
  5:        **for** each factor j connected to x_i except a **do**
  6:          $\mu^m_{x_i \to a}(\text{ state of } x_i) = \mu^m_{x_i \to a}(\text{ state of } x_i)$ $\mu_{j \to x_i}(\text{ state of } x_i)$
  7:        **end for**
  8:      **end for**
  9:      Include prior by $\mu^m_{x_i \to a}(x_i) \leftarrow \mu^m_{x_i \to a}(x_i)\varphi(x_i)$
 10:      Damp $\mu^m_{x_i \to a}(x_i)$
 11:      Normalize $\mu^m_{x_i \to a}(x_i)$
 12:      Send message $\mu^m_{x_i \to a}(x_i)$
 13:    **end for**
 14: **end for**
 15: $m \leftarrow m + 1$

Go back to step 4 if $m < m_{max}$.

6) **Marginalize:** For every variable node compute the marginal according to Eq. (21), and find the state of the variable with the highest probability.

7) **Report:** Report the highest state of each variable and construct **G**.

ACKNOWLEDGMENT

REFERENCES

[1] J. Zlotogora, "Population programs for the detection of couples at risk for severe monogenic genetic diseases," *Hum. Genet.*, vol. 126, pp. 247–253, Aug 2009.

[2] G. Rosner, S. Rosner, and A. Orr-Urtreger, "Genetic testing in Israel: an overview," *Annu Rev Genomics Hum Genet*, vol. 10, pp. 175–192, 2009.

[3] M. L. Metzker, "Emerging technologies in DNA sequencing," *Genome Res.*, vol. 15, pp. 1767–1776, Dec 2005.

[4] K. R. Chi, "The year of sequencing," *Nat. Methods*, vol. 5, pp. 11–14, Jan 2008.

[5] J. Shendure and H. Ji, "Next-generation DNA sequencing," *Nat. Biotechnol.*, vol. 26, pp. 1135–1145, Oct 2008.

[6] D. W. Craig, J. V. Pearson, S. Szelinger, A. Sekar, M. Redman, J. J. Corneveaux, T. L. Pawlowski, T. Laub, G. Nunn, D. A. Stephan, N. Homer, and M. J. Huentelman, "Identification of genetic variants using bar-coded multiplexed sequencing," *Nat. Methods*, vol. 5, pp. 887–893, Oct 2008.

[7] R. Cronn, A. Liston, M. Parks, D. S. Gernandt, R. Shen, and T. Mockler, "Multiplex sequencing of plant chloroplast genomes using Solexa sequencing-by-synthesis technology," *Nucleic Acids Res.*, vol. 36, p. e122, Nov 2008.

[8] E. Candes, J. Romberg, and T. Tao, "Robust uncertainty principles: exact signal reconstruction from highly incomplete frequency information," *Information Theory, IEEE Transactions on*, vol. 52, pp. 489–509, Feb. 2006.

[9] D. Donoho, "Compressed sensing," *Information Theory, IEEE Transactions on*, vol. 52, pp. 1289–1306, April 2006.

[10] D. Du and F. K. Hwang, *COMBINATORIAL GROUP TESTING AND ITS APPLICATIONS*. Singapore, Singapore: World Scientific, 1999.

[11] D. Du and F. K. Hwang, *POOLING DESIGNS AND NONADAPTIVE GROUP TESTING*. Singapore, Singapore: World Scientific, 2006.

[12] W. Kautz and R. Singleton, "Nonrandom binary superimposed codes," *Information Theory, IEEE Transactions on*, vol. 10, pp. 363–377, Oct 1964.

[13] W. J. Bruno, E. Knill, D. J. Balding, D. C. Bruce, N. A. Doggett, W. W. Sawhill, R. L. Stallings, C. C. Whittaker, and D. C. Torney, "Efficient pooling designs for library screening," *Genomics*, vol. 26, pp. 21–30, Mar 1995.

[14] F. Jin, T. Hazbun, G. A. Michaud, M. Salcius, P. F. Predki, S. Fields, and J. Huang, "A pooling-deconvolution strategy for biological network elucidation," *Nat. Methods*, vol. 3, pp. 183–189, Mar 2006.

[15] G. Cormode and S. Muthukrishnan, "Combinatorial algorithms for compressed sensing," in *Proceedings of Conference on Information Sciences and Systems (CISS)*, 2006. Invited submission.

[16] S. Sarvotham, D. Baron, and R. Baraniuk, "Sudocodes fast measurement and reconstruction of sparse signals," in *IEEE International Symposium on Information Theory*, pp. 2804–2808, July 2006.

[17] A. Gilbert, M. A. Iwen, and M. J. Strauss, "Group testing and sparse signal recovery," in *42nd Asilomar Conference on Signals, Systems, and Computers, Monterey, CA, (2008).*, 2008'.

[18] M. Sheikh, O. Milenkovic, and R. Baraniuk, "Designing compressive sensing dna microarrays," in *IEEE International Workshop on Computational Advances in Multi-Sensor Adaptive Processing, 2007. CAMPSAP 2007. 2nd*, pp. 141–144, Dec. 2007.

[19] W. Dai, O. Milenkovic, M. Sheikh, and R. Baraniuk, "Probe design for compressive sensing dna microarrays," in *IEEE International Conference on Bioinformatics and Biomedicine, 2008. BIBM '08.*, pp. 163–169, Nov. 2008.

[20] Y. Erlich, K. Chang, A. Gordon, R. Ronen, O. Navon, M. Rooks, and G. Hannon, "Dna sudokuharnessing high-throughput sequencing for multiplexed specimen analysis," *Genome Research*, 2009.

[21] S. Prabhu and I. Pe'er, "Overlapping pools for high-throughput targeted resequencing," *Genome Res.*, vol. 19, pp. 1254–1261, Jul 2009.

[22] N. Shental, A. Amir, and O. Zuk, "Rare-Allele Detection Using Compressed Se(que)nsing," *arXiv*, Sep 2009, 0909.0400v1.

[23] N. Passon, F. Pozzo, C. Molinis, E. Bregant, C. Gellera, G. Damante, and R. I. Lonigro, "A simple multiplex real-time PCR methodology for the SMN1 gene copy number quantification," *Genet Test Mol Biomarkers*, vol. 13, pp. 37–42, Feb 2009.

[24] L. Hartwell, M. G. L. Hood, A. Reynolds, L.Silver, and R. Veres, *Genetics: From Genes to Genomes*. NY, USA: McGraw-Hill, 2004.

[25] J. L. Bobadilla, M. Macek, J. P. Fine, and P. M. Farrell, "Cystic fibrosis: a worldwide analysis of CFTR mutations–correlation with incidence data and application to screening," *Hum. Mutat.*, vol. 19, pp. 575–606, Jun 2002.

[26] S. Orgad, S. Neumann, R. Loewenthal, I. Netanelov-Shapira, and E. Gazit, "Prevalence of cystic fibrosis mutations in Israeli Jews," *Genet. Test.*, vol. 5, pp. 47–52, 2001.

[27] O. W. W. S.T., "A decade of molecular studies of fragile X syndrome," *Annu. Rev. Neurosci.*, vol. 25, pp. 315–338, Mar 2002.

[28] T. E. Druley, F. L. Vallania, D. J. Wegner, K. E. Varley, O. L. Knowles, J. A. Bonds, S. W. Robison, S. W. Doniger, A. Hamvas, F. S. Cole, J. C. Fay, and R. D. Mitra, "Quantification of rare allelic variants from pooled genomic DNA," *Nat. Methods*, vol. 6, pp. 263–265, Apr 2009.

[29] D. R. Bentley, S. Balasubramanian, H. P. Swerdlow, G. P. Smith, J. Milton, C. G. Brown, K. P. Hall, D. J. Evers, C. L. Barnes, H. R. Bignell, J. M. Boutell, J. Bryant, R. J. Carter, R. Keira Cheetham, A. J. Cox, D. J. Ellis, M. R. Flatbush, N. A. Gormley, S. J. Humphray, L. J. Irving, M. S. Karbelashvili, S. M. Kirk, H. Li, X. Liu, K. S. Maisinger, L. J. Murray, B. Obradovic, T. Ost, M. L. Parkinson, M. R. Pratt, I. M. Rasolonjatovo, M. T. Reed, R. Rigatti, C. Rodighiero, M. T. Ross, A. Sabot, S. V. Sankar, A. Scally, G. P. Schroth, M. E. Smith, V. P. Smith, A. Spiridou, P. E. Torrance, S. S. Tzonev, E. H. Vermaas, K. Walter, X. Wu, L. Zhang, M. D. Alam, C. Anastasi, I. C. Aniebo, D. M. Bailey, I. R. Bancarz, S. Banerjee, S. G. Barbour, P. A. Baybayan, V. A. Benoit, K. F. Benson, C. Bevis, P. J. Black, A. Boodhun, J. S. Brennan, J. A. Bridgham, R. C. Brown, A. A. Brown, D. H. Buermann, A. A. Bundu, J. C. Burrows, N. P. Carter, N. Castillo, M. Chiara E Catenazzi, S. Chang, R. Neil Cooley, N. R. Crake, O. O. Dada, K. D. Diakoumakos, B. Dominguez-Fernandez, D. J. Earnshaw, U. C. Egbujor, D. W. Elmore, S. S. Etchin, M. R. Ewan, M. Fedurco, L. J. Fraser, K. V. Fuentes Fajardo, W. Scott Furey, D. George, K. J. Gietzen, C. P. Goddard, G. S. Golda, P. A. Granieri, D. E. Green, D. L. Gustafson, N. F. Hansen, K. Harnish, C. D. Haudenschild, N. I. Heyer, M. M. Hims, J. T. Ho, A. M. Horgan, K. Hoschler, S. Hurwitz, D. V. Ivanov, M. Q. Johnson, T. James, T. A. Huw Jones, G. D. Kang, T. H. Kerelska, A. D. Kersey, I. Khrebtukova, A. P. Kindwall, Z. Kingsbury, P. I. Kokko-Gonzales, A. Kumar, M. A. Laurent, C. T. Lawley, S. E. Lee, X. Lee, A. K. Liao, J. A. Loch, M. Lok, S. Luo, R. M. Mammen, J. W. Martin, P. G. McCauley, P. McNitt, P. Mehta, K. W. Moon, J. W. Mullens, T. Newington, Z. Ning, B. Ling Ng, S. M. Novo, M. J. O'Neill, M. A. Osborne, A. Osnowski, O. Ostadan, L. L. Paraschos, L. Pickering, A. C. Pike, A. C. Pike, D. Chris Pinkard, D. P. Pliskin, J. Podhasky, V. J. Quijano, C. Raczy, V. H. Rae, S. R. Rawlings, A. Chiva Rodriguez, P. M. Roe, J. Rogers, M. C. Rogert Bacigalupo, N. Romanov, A. Romieu, R. K. Roth, N. J. Rourke, S. T. Ruediger, E. Rusman, R. M. Sanches-Kuiper, M. R. Schenker, J. M. Seoane, R. J. Shaw, M. K. Shiver, S. W. Short, N. L. Sizto, J. P. Sluis, M. A. Smith, J. Ernest Sohna Sohna, E. J. Spence, K. Stevens, N. Sutton, L. Szajkowski, C. L. Tregidgo, G. Turcatti, S. Vandevondele, Y. Verhovsky, S. M. Virk, S. Wakelin, G. C. Walcott, J. Wang, G. J. Worsley, J. Yan, L. Yau, M. Zuerlein, J. Rogers, J. C. Mullikin, M. E. Hurles, N. J. McCooke, J. S. West, F. L. Oaks, P. L. Lundberg, D. Klenerman, R. Durbin, and A. J. Smith, "Accurate whole human genome sequencing using reversible terminator chemistry," *Nature*, vol. 456, pp. 53–59, Nov 2008.

[30] J. Aitchison, *The statistical analysis of compositional data*. London, UK, UK: Chapman & Hall, Ltd., 1986.

[31] W. H. Mow, "Recursive constructions of detecting matrices for multiuser coding: A unifying approach," *Information Theory, IEEE Transactions on*, vol. 55, pp. 93–98, Jan. 2009.

[32] P. Mathys, "A class of codes for a t active users out of n multiple-access communication system," *Information Theory, IEEE Transactions on*, vol. 36, pp. 1206–1219, Nov 1990.

[33] S.-C. Chang and E. Weldon, "Coding for t-user multiple-access channels," *Information Theory, IEEE Transactions on*, vol. 25, pp. 684–691, Nov 1979.

[34] G. Khachatrian and S. Martirossian, "Code construction for the t-user noiseless adder channel," *Information Theory, IEEE Transactions on*, vol. 44, pp. 1953–1957, Sep 1998.

[35] M. Hamady, J. J. Walker, J. K. Harris, N. J. Gold, and R. Knight, "Error-correcting barcoded primers for pyrosequencing hundreds of samples in multiplex," *Nat. Methods*, vol. 5, pp. 235–237, Mar 2008.

[36] Y. Erlich, P. P. Mitra, M. delaBastide, W. R. McCombie, and G. J. Hannon, "Alta-Cyclic: a self-optimizing base caller for next-generation sequencing," *Nat. Methods*, vol. 5, pp. 679–682, Aug 2008.

[37] A. D'yachkov, J. Macula, A.J., and V. Rykov, "New constructions of superimposed codes," *Information Theory, IEEE Transactions on*, vol. 46, pp. 284–290, Jan 2000.

[38] S. Sarvotham, D. Baron, and R. G. Baraniuk, "Measurements vs. bits: Compressed sensing meets information theory," in *Proceedings of the 44th Allerton Conference on Communication, Control, and Computing.*, 2006.

[39] D. Eppstein, M. T. Goodrich, and D. S. Hirschberg, "Improved combinatorial group testing for real-world problem sizes." ACM Computing Research Repository, May 2005, cs.DS/0505048.

[40] F. Kschischang, B. Frey, and H.-A. Loeliger, "Factor graphs and the sum-product algorithm," *Information Theory, IEEE Transactions on*, vol. 47, pp. 498–519, Feb 2001.

[41] J. Pearl, *Probabilistic Reasoning in Intelligent Systems : Networks of Plausible Inference*. Morgan Kaufmann, September 1988.

[42] C. M. Bishop, *Pattern Recognition and Machine Learning (Information Science and Statistics)*. Springer, August 2006.

[43] B. J. Frey and D. J. C. MacKay, "A revolution: belief propagation in graphs with cycles," in *NIPS '97: Proceedings of the 1997 conference on Advances in neural information processing systems 10*, (Cambridge, MA, USA), pp. 479–485, MIT Press, 1998.

[44] M. Mzard and A. Montanari, *Information, Physics, and Computation*. Oxford Graduate Texts, Oxford University Press, 2009.

[45] L. Kroc, A. Sabharwal, and B. Selman, "Message-passing and local heuristics as decimation strategies for satisfiability," in *sac09*, (Honolulu, HI), pp. 1408–1414, Mar. 2009.

[46] T. Moon and J. Gunther, "Multiple constraint satisfaction by belief propagation: An example using sudoku," in *IEEE Mountain Workshop on Adaptive and Learning Systems*, pp. 122–126, July 2006.

[47] M. Mézard and M. Tarzia, "Statistical mechanics of the hitting set problem," *Physical Review E*, vol. 76, no. 4, pp. 041124+, 2007.

[48] D. Baron, S. Sarvotham, and R. G. Baraniuk, "Bayesian compressive sensing via belief propagation," Dec 2008, 0812.4627.

[49] M. Pretti, "A message-passing algorithm with damping," *Journal of Statistical Mechanics: Theory and Experiment*, vol. 2005, pp. P11008+, November 2005.